

## Basicity of Coordinated Pyrazine and Bonding Interactions with $[M^{II}(\text{CN})_5]^{3-}$ Fragments (M = Fe, Ru, Os)

Leonardo D. Slep, Sergio Pollak, and José A. Olabe\*

Departamento de Química Inorgánica, Analítica y Química Física, INQUIMAE, Facultad de Ciencias Exactas y Naturales, Universidad de Buenos Aires, Pabellón 2, Ciudad Universitaria, Buenos Aires 1428, República Argentina

Received March 1, 1999

### Introduction

Modification of the basicity of pyrazine (pz) upon coordination to  $[\text{MX}_5]$  fragments was related to the back-bonding capabilities of the latter species.<sup>1</sup> Saturated coligands such as amines change the  $\text{p}K_a$  of free  $\text{pzH}^+$  (0.6) to 2.5 and 7.4 for M = Ru(II)<sup>2</sup> and Os(II)<sup>3</sup>, respectively. The  $\text{p}K_a$  values depend on the bonding properties of the coligands for a given metal, as shown by the upward and downward shifts for  $[\text{Os}^{II}\text{A}_5\text{pzH}]^{3+}$  (A = ammine) when one of the A ligands is substituted by a  $\pi$ -donor (chloride) or a  $\pi$ -acceptor (dinitrogen) ligand, respectively.<sup>4</sup>

A current interest exists in establishing the bonding trends for the  $[\text{M}^{II}(\text{CN})_5\text{L}]^{n-}$  series (M = Fe, Ru, Os).<sup>5–8</sup> The  $\text{p}K_a$  values quoted for L =  $\text{pzH}^+$  in the iron (0.065) and ruthenium (0.4) complexes were composite values, associated to competitive and successive equilibria on pyrazine and cyanides. These results disagreed with NMR measurements, suggesting that iron could be more strongly back-bonding than ruthenium,<sup>7</sup> a result substantiated later for the L = dimethylpyrazine derivatives.<sup>9</sup>

After the synthesis of the  $[\text{Os}^{II}(\text{CN})_5\text{pz}]^{3-}$  ion,<sup>8a</sup> it seemed worthwhile to extend the basicity studies and revisit the titration experiments with the iron and ruthenium analogues. Using an adequate acid–base description and a chemometrical methodology,<sup>10</sup> we present  $\text{p}K_a$  values for the mono- and diprotonated species in the three complexes, disclosed UV–visible spectra and reliable separate  $\text{p}K_a$  values for the pz- and cyanide-protonated species. Complementary NMR measurements support the analysis of the bonding trends for the  $[\text{M}^{II}(\text{CN})_5\text{pz}]^{3-}$  species.

\* Corresponding author. Fax: 54 11-4576-3341. E-mail: olabe@q3.fcen.uba.ar.

- (1) (a) Taube, H. *Surv. Prog. Chem.* **1973**, 6, 1. (b) Taube, H. *Pure Appl. Chem.* **1979**, 51, 901.
- (2) Ford, P.; Rudd, D. P.; Gaunders, R.; Taube, H. *J. Am. Chem. Soc.* **1968**, 90, 1187.
- (3) Sen, J.; Taube, H. *Acta Chem. Scand.* **1979**, A33, 125.
- (4) Magnuson, R. H.; Taube, H. *J. Am. Chem. Soc.* **1975**, 97, 5129.
- (5) Macartney, D. H. *Rev. Inorg. Chem.* **1988**, 9, 101.
- (6) Toma, H. E.; Malin, J. M. *Inorg. Chem.* **1973**, 12, 1039.
- (7) Johnson, C. R.; Shepherd, R. E. *Inorg. Chem.* **1983**, 22, 1117.
- (8) (a) Slep, L. D.; Baraldo, L. M.; Olabe, J. A. *Inorg. Chem.* **1996**, 35, 6327. (b) Waldhör, E.; Kaim, W.; Olabe, J. A.; Slep, L. D.; Fiedler, J. *Inorg. Chem.* **1997**, 36, 2969.
- (9) Toma, H. E.; Stadler, E. *Inorg. Chem.* **1985**, 24, 3085.
- (10) (a) Malinowski, E. R. *Factor Analysis in Chemistry*, 2nd ed.; Wiley-Interscience: New York, 1991. (b) Parise, A. R.; Pollak, S.; Slep, L. D.; Olabe, J. A. *An. Asoc. Quim. Argent.* **1995**, 83, 211. (c) Stultz, L. K.; Binstead, R. A.; Reynolds, M. S.; Meyer, T. J. *J. Am. Chem. Soc.* **1995**, 117, 2520.

### Experimental Section

**Salts of the Pentacyano-L Complexes.**  $\text{Na}_3[\text{Fe}(\text{CN})_5\text{pz}] \cdot 4\text{H}_2\text{O}$ ,  $\text{K}_3[\text{Ru}(\text{CN})_5\text{pz}] \cdot x\text{H}_2\text{O}$ , and  $\text{Na}_3[\text{Os}(\text{CN})_5\text{L}] \cdot x\text{H}_2\text{O}$  (L = py, pz, dmpz, *N*-methylpyrazinium (mepz<sup>+</sup>)) were prepared as previously described.<sup>6,8</sup> All other chemicals were of analytical grade. NMR spectra were recorded on a Bruker AC200 spectrometer. The  $\text{p}K_a$ s for the different protonation equilibria were determined spectrophotometrically with a Hewlett-Packard 8452A instrument. Solutions containing weighed amounts of the corresponding salts of the  $[\text{M}(\text{CN})_5\text{pz}]^{3-}$  ions (around  $10^{-5}$  M) and varying concentrations of HCl were prepared (pH range 0–7,  $I = 1$  M, NaCl). The UV–vis spectra were obtained quickly after adding the acid and diluting to volume, using a 10.00 cm quartz cuvette. Repetitive scans were performed on each solution to ensure stability under acid conditions.

An adequate characterization of the species in solution was achieved by using the SPECFIT software package. It consists of a global least-squares fitting routine for equilibrium and kinetics experiments that uses factor-analysis decomposition methods;<sup>10</sup> this was useful to obtain the single species' spectra along with the equilibrium constants.

### Results and Discussion

Figure 1 shows the titration spectra for the  $[\text{M}^{II}(\text{CN})_5\text{pz}]^{3-}$  complexes. For the three metals the behavior is similar, showing multistep protonation: Figure 1a shows the spectra of solutions of  $\text{Na}_3[\text{Fe}(\text{CN})_5\text{pz}] \cdot 4\text{H}_2\text{O}$ . The MLCT band at 452 nm<sup>6</sup> decays for decreasing pH's, while new bands develop at 408 and 636 nm, with isosbestic points at 272, 321, 418, and 544 nm (range 7.0–2.0). In the pH range 2.0–0.0 the isosbestic points disappear and the maxima of both bands shift to lower wavelengths (378 and 556 nm). The ruthenium (and osmium) complexes display similar behavior. Figure 1b (1c) shows that when going from pH 7 to 2 the MLCT bands at 372<sup>7</sup> (384)<sup>8a</sup> nm decay, being replaced by two absorptions at 342 (345) and 504 (514) nm. Upon further acidification these bands are replaced by new absorptions at 322 (315) and 444 (460) nm.

For the three metals, the factor analysis displays *only* three colored species, consistent with a two-step protonation scheme:



The concentration profiles depending on  $[\text{H}^+]$  are given by

$$[\text{M}^{II}(\text{CN})_5\text{pz}] = \frac{C_0 K_1 K_2}{[\text{H}^+]^2 + K_2[\text{H}^+] + K_1 K_2} \quad (1)$$

$$[\text{M}^{II}(\text{CN})_5\text{pz}] \text{H} = \frac{C_0 [\text{H}^+] K_2}{[\text{H}^+]^2 + K_2[\text{H}^+] + K_1 K_2} \quad (2)$$

$$[\text{M}^{II}(\text{CN})_5\text{pz}] \text{H}_2 = \frac{C_0 [\text{H}^+]^2}{[\text{H}^+]^2 + K_2[\text{H}^+] + K_1 K_2} \quad (3)$$

Leaving  $K_1$  and  $K_2$  as fitting parameters, we retrieve the spectra of the three species (displayed as insets in Figure 1) and the following results for  $\text{p}K_1$ :  $1.84 \pm 0.05$  (Fe),  $1.44 \pm 0.05$  (Ru),  $1.88 \pm 0.04$  (Os). For  $\text{p}K_2$  we obtain  $0.4 \pm 0.1$  (Fe),  $0.3 \pm 0.6$  (Ru),  $-0.2 \pm 0.6$  (Os).

These  $\text{p}K_1$  and  $\text{p}K_2$  values do not reflect clean, separated protonation steps at pz or cyanide ligands. The *two* new MLCT

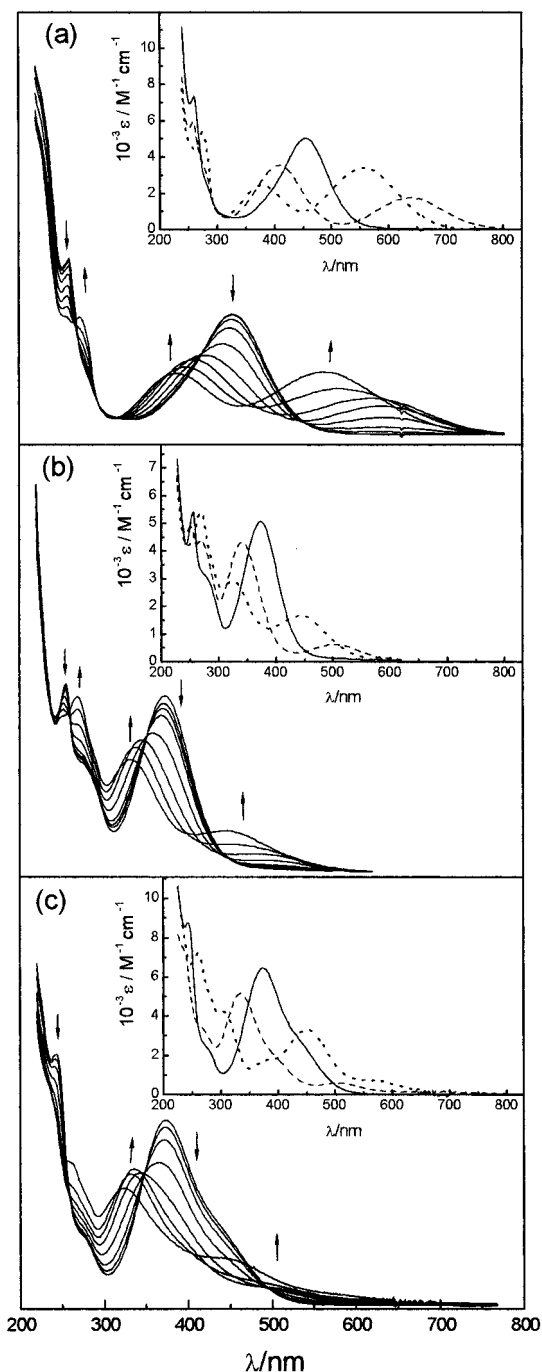
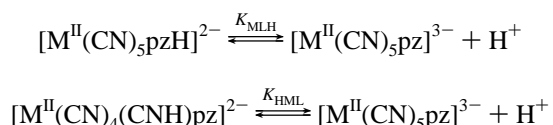


**Figure 1.** Spectrophotometric acid–base titration of the  $[\text{M}^{\text{II}}(\text{CN})_5\text{pz}]^{3-}$  complexes ((a), (b), (c) correspond to Fe, Ru, Os, respectively),  $c = \text{ca. } 1 \times 10^{-5} \text{ M}$ ,  $I = 1 \text{ M}$  (NaCl), pH range = 0–7 (HCl). Arrows indicate the changes observed on increasing acidity of the medium. Insets: Spectra obtained for the un-, mono-, and diprotonated species (full, dashed, dotted lines, respectively).

bands in the monoprotonated species spectra show that *both* pz and cyanide are affected by the *first* protonation step.



The concentration ratio of monoprotonated species is pH independent, hence behaving as a pure monoprotonated moiety, with a *global* acidity constant  $K_1$ , related to the *individual*  $K_{\text{HML}}$

**Table 1.** Absorption Maxima (nm), Disclosed Individual  $\text{p}K_{\text{a}}$  Values, and  $^1\text{H}$  NMR Chemical Shifts for  $[\text{M}(\text{CN})_5\text{pz}]^{3-}$  Systems

	Fe	Ru	Os
$\lambda_{\text{max}}([\text{M}(\text{CN})_5\text{pz}]^{3-})^a$	452 (5011)	372 (5040)	384 (6435)
$\lambda_{\text{max}}([\text{M}(\text{CN})_5\text{pzH}]^{2-})^b$	636 (6900)	504 (6540)	514 (12700)
$\Delta E \text{ (cm}^{-1}\text{)}^c$	6400	7040	6600
$\lambda_{\text{max}}([\text{(HNC)M}(\text{CN})_4\text{pz}]^{2-})^d$	408 (4710)	342 (4750)	345 (5380)
$\lambda_{\text{max}}([\text{(HNC)M}(\text{CN})_4\text{pzH}]^{-})$	556	444	460
$\lambda_{\text{max}}([\text{(HNC)}_2\text{M}(\text{CN})_3\text{pz}]^{-})$	378	322	315
$\text{p}K_{\text{MLH}}^e$	$1.24 \pm 0.07^f$	$0.41 \pm 0.06^f$	$0.53 \pm 0.05$
$\text{p}K_{\text{HML}}^e$	$1.71 \pm 0.09$	$1.40 \pm 0.06$	$1.86 \pm 0.04$
$\delta(\text{CH})\alpha^g$	$9.09^h$	$8.72, \text{dd}^{h,i}$	$9.11, \text{dd}^j$
$\delta(\text{CH})\beta^g$	$8.24^h$	$8.45, \text{dd}^{h,i}$	$8.36, \text{dd}^j$

<sup>a</sup> Values in parentheses are the molar absorptances  $\epsilon \text{ (M}^{-1} \text{cm}^{-1}\text{)}$ .

<sup>b</sup> Values in parentheses are estimated molar absorptances (see text).

<sup>c</sup> Energy difference between the absorption maxima for  $[\text{M}(\text{CN})_5\text{pz}]^{3-}$  and  $[\text{M}(\text{CN})_5\text{pzH}]^{2-}$ . <sup>d</sup> Molar absorptances calculated according to eq 5. <sup>e</sup> This work,  $I = 1 \text{ M}$ ,  $25 \text{ }^\circ\text{C}$ . <sup>f</sup> 0.065 (Fe); 0.4 (Ru), in ref 7.

<sup>g</sup>  $\delta$  (ppm) in  $\text{D}_2\text{O}$  vs TMS. Data for free pz: 8.69. Data for  $[\text{Co}^{\text{III}}(\text{CN})_5\text{pz}]^{2-}$ : 8.99( $\alpha$ ), 8.72( $\beta$ ). <sup>h</sup> Reference 7. <sup>i</sup>  $\text{A}_2\text{X}_2$  system, with  $^3J_{\text{H}_\alpha\text{H}_\beta} = 3.3 \text{ Hz}$  and  $^5J_{\text{H}_\alpha\text{H}_\beta} = 1.3 \text{ Hz}$ . <sup>j</sup>  $\text{A}_2\text{X}_2$  system, with  $^3J_{\text{H}_\alpha\text{H}_\beta} = 3.0 \text{ Hz}$  and  $^5J_{\text{H}_\alpha\text{H}_\beta} = 1.5 \text{ Hz}$ .

and  $K_{\text{MLH}}$  by

$$K_1 = \frac{K_{\text{MLH}}K_{\text{HML}}}{K_{\text{MLH}} + K_{\text{HML}}} \quad (4)$$

The individual species contribute to the observed spectra according to

$$\epsilon_{\text{obs}}(\lambda) = \frac{K_{\text{HML}}\epsilon_{\text{MLH}}(\lambda) + K_{\text{MLH}}\epsilon_{\text{HML}}(\lambda)}{K_{\text{MLH}} + K_{\text{HML}}} \quad (5)$$

In other words, even if protonation can take place at *two* nonequivalent positions, the spectrophotometric titration experiment reveals *one* “monoprotonated” species, whose spectrum is a combination of the corresponding cyano- and pz-protonated ones. Analogously, the spectra of the “diprotonated” species are combinations of those of  $[\text{(HNC)M}(\text{CN})_4\text{pzH}]^{-}$  and  $[\text{(HNC)}_2\text{M}(\text{CN})_3\text{pz}]^{-}$ .

Independent values of  $\text{p}K_{\text{MLH}}$  and  $\text{p}K_{\text{HML}}$  can be calculated from the  $\text{p}K_1$  values by estimation of the molar absorptances of the  $[\text{M}^{\text{II}}(\text{CN})_5\text{pzH}]^{2-}$  species (Table 1).<sup>11</sup> The reliability of the global  $\text{p}K_{\text{a}}$  values is supported by the analysis of the resolved spectra (insets, Figure 1). The MLCT bands of the  $[\text{M}^{\text{II}}(\text{CN})_5\text{pz}]^{3-}$  species split into two separate absorptions upon protonation. We assign the bathochromically and hypsochromically shifted bands to the  $[\text{M}^{\text{II}}(\text{CN})_5\text{pzH}]^{2-}$  and  $[\text{(HNC)M}^{\text{II}}(\text{CN})_4\text{pz}]^{2-}$  complexes, respectively.<sup>6</sup> The calculated molar absorptances are greater (pz) and smaller (cyanide) than for the corresponding unprotonated species, as expected.<sup>6</sup>

Table 1 shows that the energy differences for the unprotonated and pz-protonated MLCT bands ( $\Delta E$ ) are around 6000–7000  $\text{cm}^{-1}$ , but depend significantly on M, namely:  $\Delta E(\text{Fe}) < \Delta E(\text{Os}) < \Delta E(\text{Ru})$ . In the limit of no mixing between the M and  $\pi^*(\text{L})$  orbitals, the  $\Delta E$  values should be independent of M, corresponding to the energy differences of  $\pi^*(\text{L})$  for the pz and  $\text{pzH}^+$  ligands. The observed  $\Delta E$  values are indicative of back-bonding, decreasing in the sense  $\text{Fe} > \text{Os} > \text{Ru}$ . The sensitivity of the MLCT band energy to changes in L (or M) decreases

(11) The molar absorptances for the  $[\text{M}^{\text{II}}(\text{CN})_5\text{pzH}]^{2-}$  species were interpolated by plotting  $\log(\epsilon_{\text{MLCT}})$  (the energy of the MLCT bands) against the molar absorptance of the corresponding absorptions for a series of  $[\text{M}^{\text{II}}(\text{CN})_5\text{L}]^{n-}$  complexes ( $\text{M} = \text{Fe, Ru, Os}$ ). Then the values of  $\epsilon$  for the  $[\text{M}^{\text{II}}(\text{CN})_4(\text{CNH})\text{pz}]^{2-}$  species were obtained (eq 5).

when the back-bonding interaction between M and  $\pi^*(L)$  increases.<sup>1</sup> Besides, inspection of the individual  $pK_{MLH}$  (Table 1) and of the chemical shifts for the  $\beta$ -protons in the pz-ring<sup>12,13</sup> indicate the same trend. All this evidence suggests a decrease in back-donation to pz when going from Fe to Os and Ru.

Table 1 also shows the  $pK_{HML}$  values for the cyanide-monoprotonated species, with Os > Fe > Ru. Now the osmium center appears as the most basic, probably reflecting the synergistically behaved, strong  $\sigma$ - and  $\pi$ -interactions between osmium and cyanides, dominant in the overall bonding scheme.<sup>8a</sup> Note that this is also the order of NMR chemical shifts for the pz  $\alpha$ -protons.<sup>12-14</sup>

Although none of our measurements gives a quantitative approach to individual  $\sigma$ - or  $\pi$ - contributions, we consider that  $\pi$ -interactions are determinant of the Fe–Os–Ru order found for the  $pK_a$  values, electronic and NMR ( $\beta$ ) shifts of bound  $pzH^+$ . The  $\pi$ -interaction with pz appears as the strongest for iron, suggesting a dominant influence of the more favorable energy match between  $d_{Fe}$  and  $\pi^*_{pz}$  orbitals over the lesser overlapping capability of the 3d orbitals.<sup>15</sup>

- (12) Shepherd, R. E.; Chen, Y.; Johnson, C. R. *Inorg. Chim. Acta* **1998**, 267, 11.
- (13) Upfield chemical shifts for the  $\beta$ -protons and downfield shifts for the  $\alpha$ -protons seem to be characteristic of *N*-heterocyclic ligands in negatively charged  $MX_5$  moieties.<sup>12</sup> A second-order influence of the  $\sigma$ - $\pi$  interactions also operates at the  $\alpha$ -positions; however, the  $\beta$  (and  $\gamma$ ) positions show to be more sensitive to  $\pi$ -back-bonding, because of attenuation of the  $\sigma$ -interactions with distance. For  $[Co^{III}(CN)_5pz]^{2-}$  (no back-bonding and lower overall charge than the others), both  $\alpha$ - and  $\beta$ -protons shift downfield (Table 1), as was the case with the 2-Mepz complexes;<sup>12</sup> thus, the upfield shifts for the Fe, Ru, and Os pz-complexes seem to be really traced to the  $\pi$ -interactions.
- (14) As a check of consistency, we also made titrations with other  $[Os(CN)_5L]^{n-}$  complexes where only cyanide was protonable. The results for L = py ( $pK_a$  2.33) and L = mepz<sup>+</sup> ( $pK_a$  = 1.05), together with the pz value, show that the cyanide-basicity decreases with the  $\pi$ -acceptor capability of L, as expected (Supporting Information, Figure S1).
- (15) The values of  $E$  for the  $[M^{III}, II(CN)_5pz]^{2-, 3-}$  redox couples are: 0.55 (Fe);<sup>6</sup> 0.96 (Ru), cf. Henderson, W. W.; Shepherd, R. E. *Inorg. Chem.* **1985**, 24, 2398; 0.78 (Os).<sup>8a</sup> The extent of back-donation, Fe > Ru, was previously proposed for the dmpz-complexes.<sup>9</sup> After measuring the  $[Os(CN)_5dmpzH]^{2-}$  complex, and using data taken from Figure 1

The insets of Figure 1 (dotted lines) show the spectra of the diprotonated species, which are mixtures of the  $[M^{II}(CN)_4-(CNH)pzH]^-$  and  $[M^{II}(CN)_3(CNH)_2pz]^-$  ions. Their corresponding bands are both shifted to lower wavelengths compared to the associated monoprotonated ions (dashed lines), as expected. The global  $pK_2$  values are also consistent, although a calculation of individual  $pK$  values (around zero) is associated to large errors.

As a conclusion, the basicities at the exposed end of pz or cyanides are slightly dependent on M; the  $pK_a$  order Fe > Os > Ru, agrees with the NMR results. The  $pK_a$  values for M = Ru and Os are significantly smaller than those found for the  $[M^{II}(NH_3)_5pz]^{2+}$  ions (see above),<sup>2,3</sup> reflecting the competitive influence of the cyanide coligands, as addressed by our recent calculations on the pz-basicities for the  $[Ru(CN)_5pz]^{3-}$  and  $[Ru(NH_3)_5pz]^{2+}$  aqueous species, and the increased Mulliken population on the  $\pi^*_{pz}$  orbital for the latter compound.<sup>16</sup>

**Acknowledgment.** This work was supported by the University of Buenos Aires (UBA, Research Grant EX 116), the Consejo Nacional de Investigaciones Científicas y Técnicas (CONICET), and the Deutsche Gesellschaft für Zusammenarbeit GmbH. L.D.S. was a member of the Graduate Fellowship Program of UBA, and J.A.O. is a member of the research staff of CONICET. We thank Dr. Robert A. Binstead, of Spectrum Software Associates, Chapel Hill, NC, for providing access to the Specfit Program.

**Supporting Information Available:** Figures showing spectrophotometric acid–base titrations of  $[Os(CN)_5L]^{n-}$  ions (L = py, mepz<sup>+</sup>) and  $[M(CN)_5dmpz]^{3-}$  ions (M = Fe, Ru, Os). This material is available free of charge via the Internet at <http://pubs.acs.org>.

IC990250K

in ref 9, we found 2.68 (Fe), 1.51 (Ru), and 1.99 (Os) for the  $pK_a$  values i.e., the same order of basicities as found with the pz-complexes. The numbers for Fe and Ru are slightly different from those of ref 9, due to the adequate consideration of simultaneous cyanide protonation in the present work (Supporting Information, Figure S2).

- (16) Hamra, O. Y.; Slep, L. D.; Olabe, J. A.; Estrin, D. A. *Inorg. Chem.* **1998**, 37, 2033.